Cell Research (2009) 19:1062-1078.

www.nature.com/cr

ORIGINAL ARTICLE

PrP^C-related signal transduction is influenced by copper, membrane integrity and the alpha cleavage site

Cathryn L Haigh[1, 2], Victoria A Lewis[1, 2], Laura J Vella[1, 2, 4], Colin L Masters[2, 5], Andrew F Hill[2, 3, 4], Victoria A Lawson[1, 2], Steven J Collins[1, 2]

[1]Department of Pathology; [2]Mental Health Research Institute; [3]The Department of Biochemistry and Molecular Biology; [4]Bio21 Molecular Science and Biotechnology Institute, 30 Flemington Road; [5]Centre for Neuroscience, The University of Melbourne, Parkville, Melbourne, 3010, Australia

The copper-binding, membrane-anchored, cellular prion protein (PrP^C) has two constitutive cleavage sites producing distinct N- and C-terminal fragments (N1/C1 and N2/C2). Using RK13 cells expressing either human PrP^C, mouse PrP^C or mouse PrP^C carrying the 3F4 epitope, this study explored the influence of the PrP^C primary sequence on endoproteolytic cleavage and one putative PrP^C function, MAP kinase signal transduction, in response to exogenous copper with or without a perturbed membrane environment. PrP^C primary sequence, especially that around the N1/C1 cleavage site, appeared to influence basal levels of proteolysis at this location and extracellular signal-regulated kinase 1/2 (ERK1/2) phosphorylation, with increased processing demonstrating an inverse relationship with basal ERK1/2 activation. Human PrP^C showed increased N1/C1 cleavage in response to copper alone, accompanied by specific p38 and JNK/SAPK phosphorylation. Combined exposure to copper plus the cholesterol-sequestering antibiotic filipin resulted in a mouse PrP^C-specific substantial increase in signal protein phosphorylation, accompanied by an increase in N1/C1 cleavage. Mouse PrP^C harboring the human N1/C1 cleavage site assumed more human-like profiles basally and in response to copper and altered membrane environments. Our results demonstrate that the PrP^C primary sequence around the N1/C1 cleavage site influences endoproteolytic processing at this location, which appears linked to MAP kinase signal transduction both basally and in response to copper. Further, the primary sequence appears to confer a mutual dependence of N1/C1 cleavage and membrane integrity on the fidelity of PrP^C-related signal transduction in response to exogenous stimuli.

***Keywords*:** Prion, copper, endoproteolytic cleavage, signal transduction, lipid raft

Cell Research (2009) **19**:1062-1078. doi: 10.1038/cr.2009.86; published online 14 July 2009

Introduction

Cumulative experimental evidence supports that abnormal isomers of the prion protein constitute the causative agent in transmissible spongiform encephalopathies (TSEs, also known as prion diseases) [1, 2], with neuronal expression and membrane anchorage of wild-type PrP being essential for efficient pathogenesis [3-9]. The disease-associated conformer, termed PrP^{Sc}, is a structurally altered form of the normal cellular protein, PrP^C. PrP^C is a glycosylphosphatidylinositol (GPI)-anchored cell surface glycoprotein, which has been shown to bind copper within an N-terminal octameric repeat region and also at one or more sites slightly more C-terminal of the repeat region [10-13].

Despite much investigation and characterization of the properties of PrP^C and PrP^{Sc}, the primary function of PrP^C and the principal pathogenic pathways of TSEs remain unresolved. One suggested role for PrP^C is the transduction of signals from the external environment into the cell interior, a function circumstantially supported by the localization of PrP^C within plasma membrane detergent-resistant microdomains (also known as lipid rafts), which are now widely recognized as membrane-signaling plat-

Correspondence: Steven J Collins
Tel: +61 3 8344 1945; Fax: +61 3 9349 5105
E-mail: stevenjc@unimelb.edu.au
Received 5 November 2008; revised 10 April 2009; accepted 22 May 2009; published online 14 July 2009

forms [14]. The plasma membrane constitutes a critical site for the activation of intracellular, and transduction of extracellular, receptor-mediated signaling, and the lipid environment itself appears to play an extensive role in modulating the activation of signaling pathways [15, 16]. PrP^C has been thought to have a role in lymphocyte signal transduction for some time [17], with suggested outcomes including T-lymphocyte activation or the initiation of a proliferation response [18, 19]. PrP^C crosslinking in lymphocytes results in mitogen-activated protein kinase (MAPK) activation and subsequent extracellular signal-regulated kinase 1/2 (ERK1/2) activation [20].

PrP^C has been shown to interact with several proteins that lead to signal transduction. Co-immunoprecipitation identifies Grb2, an adaptor protein that putatively functions to link extracellular receptors to intracellular signaling molecules, as directly interacting with PrP^C [21]. Interaction with stress-inducible protein 1 (STI-1), which occurs at the cell surface mainly on the cell body, has been shown to induce neuritogenesis and neuroprotection via the MAPK pathway [22]. Additionally, clustering of PrP^C at the cell surface activates ERK1/2 [23-25]. This may be mediated by epidermal growth factor receptor (EGFR [23]) or by the signaling molecule Fyn tyrosine kinase, recruited in turn by the interaction of caveolin-1 and PrP^C [25, 26].

PrP^C is highly conserved across mammalian species, both at the primary amino acid sequence and the tertiary folded structure levels [27]. PrP^C constitutively undergoes two well-defined endoproteolytic cleavage events. The first cleavage site, termed α-cleavage and producing fragments designated N1/C1, is at amino acids 111/112 of the human PrP^C sequence (110/111 of the mouse sequence) and is known to be a site for the enzymes A Disintegrin And Metalloprotease 10 (ADAM10) and Tumor necrosis factor α-Converting Enzyme (TACE) [28]. The second cleavage site, termed β-cleavage and producing N2/C2 fragments, is around the end of the octameric repeat region, amino acid 91 of the human sequence (residue 90 of the mouse sequence), and can be caused by reactive oxygen species (ROS) without the need for enzymes [29, 30]. Enhanced N2/C2 cleavage is associated with disease [31]. Increased prominence of the C2 fragment is found in the brains of sporadic Creutzfeldt-Jakob disease patients and progressive central nervous system accumulation of this cleavage product occurs during the incubation period of rodent disease models [32]. Given the evolutionary conservation of PrP and the apparently ubiquitous occurrence of cellular endoproteolytic processing, especially alpha cleavage in the non-diseased state, it is plausible that cleavage events may be integral to both normal PrP^C function and pathogenesis.

Mouse PrP^C is often substituted for human PrP^C in studies of prion diseases due to its ability to propagate infection within cell culture systems and the availability of a bioassay to properly confirm cell culture results. There are, however, differences in the protein sequence across the two species, notably at the N1/C1 cleavage site where the human sequence contains a methionine residue at amino acid 111 as opposed to the valine residue at the equivalent position (amino acid 110) of the mouse sequence. With the exception of human, chimpanzee, macaque and some hamster species, which have the methionine residue, all characterized mammalian species have the valine residue at the N1/C1 cleavage site [27]. Since single amino acid substitutions at certain positions within the PrP^C sequence are sufficient to cause hereditary prion disease, it seems likely that even small differences in the protein sequence homology could be highly influential in PrP^C processing, function and cellular membrane interactions.

To explore potential relationships between PrP^C endoproteolytic processing and signal transduction, we developed a model in which different primary sequences notably varying around the N1/C1 cleavage motif were expressed in the same cell line. The rabbit kidney epithelial (RK13) cell line was chosen because of the absence of detectable levels of potentially confounding endogenous PrP^C and the ability to reproducibly achieve similar expression levels upon transfection of the various PrP^C constructs. For our model, intermediates of the MAP kinase signal transduction pathway were chosen for analysis because of the specific evidence for involvement of this cascade in PrP^C-related cellular activities and the general centrality of this pathway across a range of cellular signaling events. Employing this paradigm, the specific aims of the present study were: (1) to assess basal and copper-induced PrP^C cleavage profiles, especially around the N1/C1 cleavage site, and the corresponding activation states of key MAP kinase intracellular signaling intermediates and (2) to assess the effect of perturbations to plasma membrane integrity on endogenous PrP^C cleavage and the activation of key MAP kinase-signaling intermediates in response to copper across different PrP^C primary sequences. Overall, our results demonstrated a significant influence of PrP^C primary sequence around the N1/C1 cleavage site on endoproteolytic processing at this location, which appeared linked to MAP kinase signal transduction both basally and in response to copper. Further, the primary sequence appeared to confer a mutual dependence between N1/C1 cleavage and membrane integrity on the fidelity of PrP^C-related signal transduction in response to exogenous copper.

Results

Generation of cell lines expressing human or mouse PrP^C primary sequences

Human and mouse PrP^C share 89% (full-length sequence) or 91% (minus signal peptides) sequence identity (Supplementary information, Figure S1A). To investigate the influence of the species-specific differences in PrP^C amino acid sequence on cellular processing and signaling responses, basally and in response to membrane perturbations, human and mouse PrP^C genes were transfected into RK13 cells (referred to as huRK13 and moRK13 cells, respectively). The results presented encompass experiments using clones from three independent transfections where clones of equivalent expression levels were selected (Supplementary information, Figure S1B and S1C), and were, additionally, verified using an unselected mixed population. The RK13 cell line is a rabbit kidney epithelial line, which shows no detectable PrP^C and therefore represents a neutral or "null" background for expressing these genes. Furthermore, RK13 cells have been used as an effective host for the propagation of infection using transfected PrP^C sequences from various species [33, 34]. The empty vector was also transfected and selected to act as an appropriately treated control cell line (referred to as vecRK13). No difference in PrP^C detergent solubility or cell membrane localization/orientation (as determined by phosphatidylinositol-specific phospholipase C digestion) was seen between the huRK13 and moRK13 cell lines (data not shown); however, a slight difference in the mobility of the smaller fragments is apparent by western blot (Supplementary information, Figure S1B).

Human and mouse PrP^C show different basal C1 cleavage in RK13 cells

To look at the quantity of the C1 and C2 cleavage fragments compared to the full-length PrP^C molecule, PNGase F-digested cell lysates were analyzed by western blot. Blots and graphical results are shown in Figure 1A. The C2 fragment is not clearly seen in the example blots due to the much lower levels present. Densitometric quantification of the bands showed that basal N1/C1 cleavage of moPrP^C is significantly greater than that of huPrP^C. This was not true for the N2/C2 cleavage, which was not significantly different across the cell lines.

Expression of human and mouse PrP^C in RK13 cells influences ERK activation

Since PrP^C cleavage may be linked to its cellular function, and one suggested function is signal transduction, the effect of expressing human and mouse PrP^C in the RK13 cell line on basal signaling protein activation was investigated. Assessment of basal levels of phosphorylation of central signaling molecules was made by western blotting lysates of the huRK13, moRK13 and vecRK13 cells with antibodies against p-ERK1/2 and ERK1/2, p-JNK/SAPK and JNK/SAPK, and p-p38 and p38. For each antibody pair, the phosphorylated form was blotted first to avoid dephosphorylation by membrane stripping. Expression of mouse PrP^C significantly reduced basal p-ERK1/2 levels compared to those of the human PrP^C and vector-only cells (Figure 1B and 1C). Only faint signal was seen for basal phosphorylation of p38 and JNK/SAPK, and no significant alterations were observed across the three RK13 cell lines (Figure 1B). Additionally, expression of human or mouse PrP^C in the RK13 cells did not alter steady state expression of any of the signaling proteins studied.

Expression of PrP^C in RK13 cells does not alter intracellular ROS levels

Since PrP^C is linked to protection against ROS insults and ROS have been shown to be involved in PrP^C cleavage, the basal levels of ROS within the RK13 cell lines were assessed by DCFDA assay. The CM-H_2-DCFDA assay detects the ROS H_2O_2 (in the presence of endogenous metal ions only), $HO^{\cdot}$, $ROO^{\cdot}$ and $ONOO^-$ [35]. Under basal conditions there was no difference in the intracellular ROS production between the PrP^C-expressing RK13 cells and the vector-only control (Figure 1D).

Exogenous copper and altered membrane fluidity exerts a greater influence on huRK13 N1/C1 cleavage than moRK13

Since PrP^C is a plasma membrane, lipid raft-associated protein, and its localization is considered important for normal function and pathogenesis factors that alter membrane fluidity or lipid raft integrity were deemed likely to alter PrP^C membrane position, and therefore cleavage and/or PrP^C-associated intracellular signaling events. Several well-characterized conditions for altering membrane fluidity were utilized, including 10 mM benzyl alcohol (BA), to increase membrane fluidity and lowering cell temperature to 25 ºC, with or without the stiffening agent DMSO (0.5% v/v), to decrease membrane fluidity [36-38]. In addition to these conditions, 1 μM Filipin, an antibiotic that binds and sequesters cholesterol, was employed to specifically disrupt the more densely packed cholesterol-rich lipid raft domains, with the decrease in membrane cholesterol also leading to increased membrane fluidity. To confirm that these treatments were having the expected effects, we used an ANS-based assay to verify membrane fluidity (Supplementary informa-

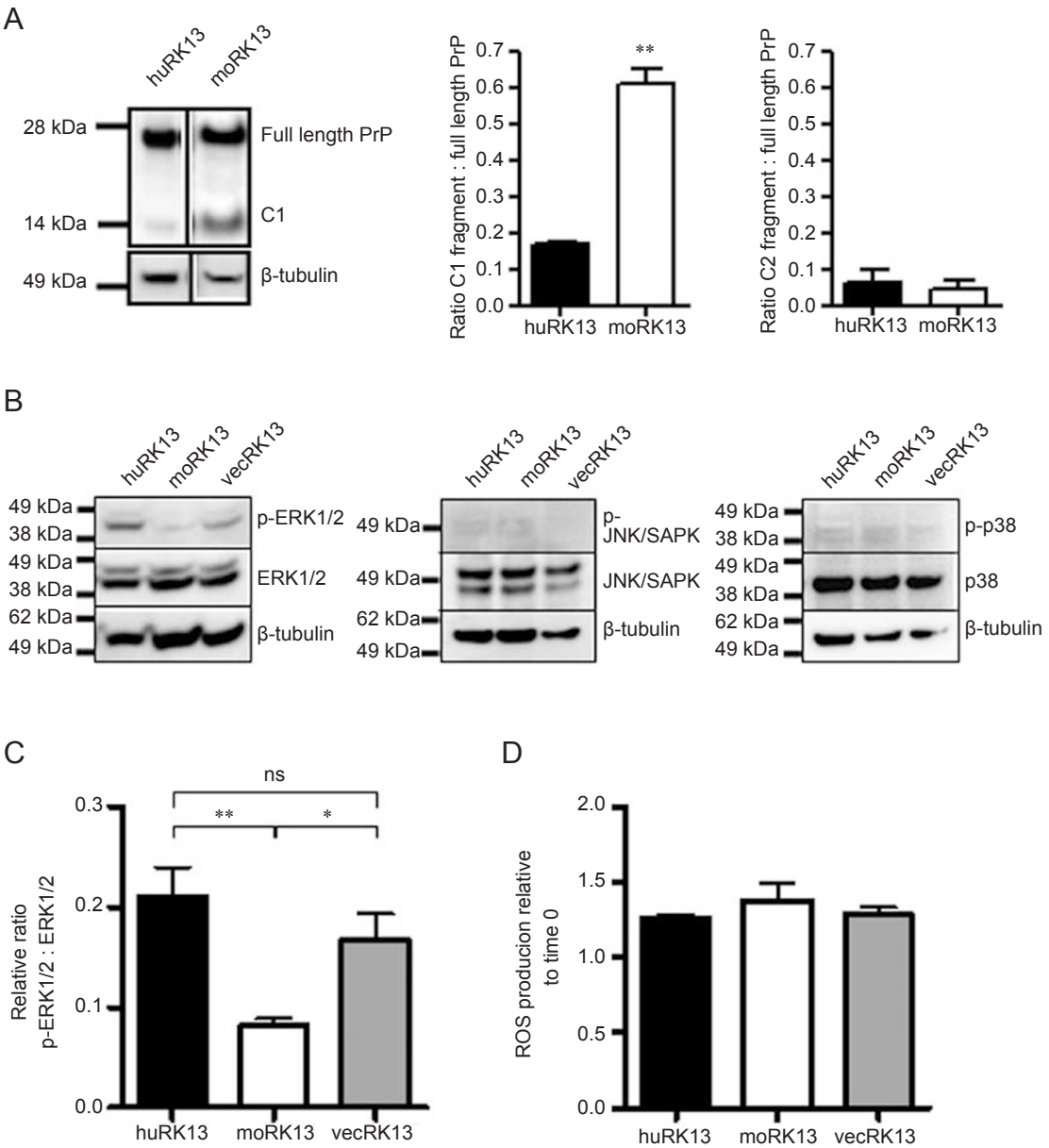

Figure 1 Basal PrP^C cleavage, MAPK activation and intracellular ROS in moRK13, huRK13 and vecRK13 cells. **(A)** Basal PrP^C cleavage of huRK13 and moRK13 cells. Lysates were PNGase F digested and western blotted with mab ICSM18 to detect the C1 fragment. β-Tubulin was blotted as a loading control. Western blots are shown on the left and densitometric quantification on the right (shown are the mean and s.e.m. of four repeats from three independently selected clones and an unselected mixed cell population). Quantification of the untreated C1 and C2 fragment band intensities is shown as a ratio to full-length PrP and reveals that moRK13 cells show significantly greater C1 cleavage compared with the huRK13 cells (t = 5.671, P = 0.0048, n = 4). No significant difference is seen between the cell lines for the C2 cleavage fragment (t = 0.368, P = 0.7328, n = 4). Western blots of basal activation of the intracellular signaling proteins ERK1/2, JNK/SAPK and p38 are shown in **(B)** and quantification of the ratio of p-ERK1/2 to ERK1/2 is shown in **(C)**. The densitometric quantification of ERK1/2 phosphorylation depicts the mean and s.e.m. of five replicates using three clones. A significant decrease in the basal level of ERK1/2 activation (phosphorylation) is observed for cells expressing $moPrP^C$ (F = 8.713, P = 0.0029, $^{**}P < 0.01$, $^{*}P < 0.05$). To assess if the expression of PrP^C within the RK13 cells alters basal ROS production, the DCFDA assay was used to quantify basal ROS **(D)**. Cells were loaded with CM-H_2-DCFDA and fluorescence was monitored at the assay start and after 30 min incubation. The plot shows the mean and s.e.m. change in fluorescence from the time 0 reading for three independently selected clones. No significant differences were seen between the cell lines by one-way ANOVA (F = 0.681, P = 0.5413). For all graphs, black, white and gray bars represent huRK13, moRK13 and vecRK13 cell line results, respectively.

tion, Figure S2). The huRK13 and moRK13 cells were exposed to increased exogenous copper and each of the conditions altered membrane fluidity both with and without copper. PrP^C is widely accepted to be a copper-binding protein. Exposing the cell lines to copper resulted in a selective increase in N1/C1 cleavage restricted to the huRK13 cells (Figure 2A); a trend toward increased N1/C1 cleavage is seen for mouse PrP but this is not significant (Figure 2B). Using BA to non-specifically increase membrane fluidity significantly altered huRK13 PrP^C N1/C1 cleavage (Figure 2A). The huRK13 N1/C1 cleavage is also increased above untreated cells for the BA plus copper treatment; however, this increase is not significantly different to the copper-alone treatment, suggesting that there is no cumulative cleavage response. The only condition to induce a significant change in moRK13 N1/C1 cleavage was the combined copper and filipin treatment; this was also significant for the huRK13 cells. Sig-

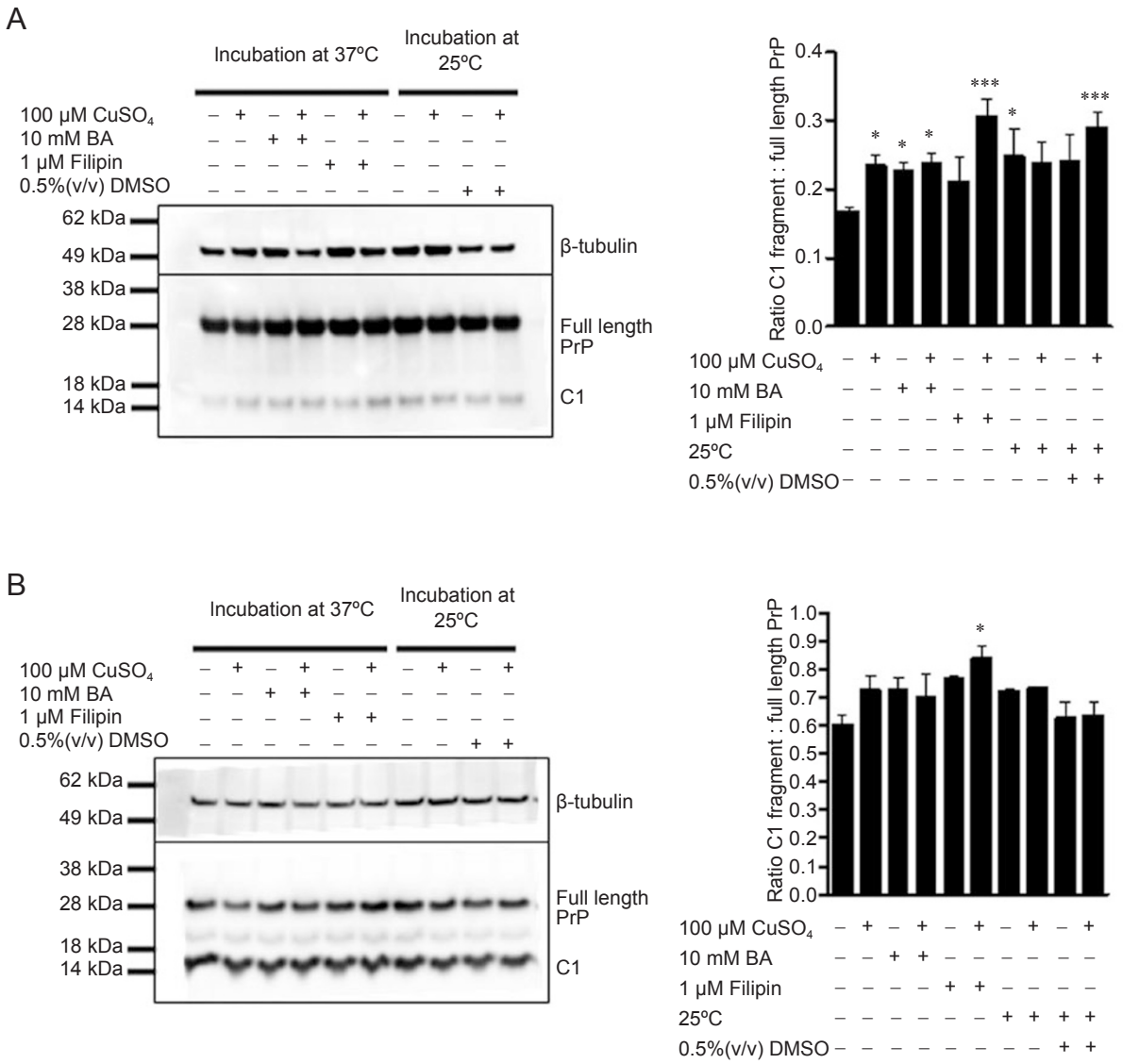

Figure 2 PrP N1/C1 cleavage profiles of the huRK13 and moRK13 cells treated with the membrane perturbing conditions with and without increased exogenous copper. HuRK13 cells **(A)** and moRK13 cells **(B)** PrP N1/C1 cleavage profile in response to treatment with each condition for 30 min before harvesting cells. Lysates were PNGase digested before electrophoresis and western blotting with mab ICSM18. Left plates show example blots and right plates show the corresponding densitometric quantification of the full-length PrP and C1 band signals with graphs representing the mean and s.e.m. of three independently selected clones. Significant differences, as determined by one-way ANOVA, are indicated by $*P < 0.05$ and $***P < 0.001$.

nificant N1/C1 cleavage within huRK13 was also seen at 25 ºC, and at 25 ºC with DMSO and increased exogenous copper.

Increased exogenous copper activates PrP^C-specific signal transduction in huRK13 cells only

Copper treatment increased ERK1/2 phosphorylation in all of the cell lines including the vecRK13 cells, indicating that copper induces a non-specific reaction via this pathway (Supplementary information, Figure S3A and S3B). A significant huRK13-specific increase in phosphorylation was seen for JNK/SAPK and p38 (Figure 3).

Global increases or decreases in membrane fluidity reduce huRK13 signal fidelity in response to copper

Increasing membrane fluidity eliminates the fidelity of the JNK/SAPK and p38 signaling response seen in the huRK13 cells (Figure 3). The phosphorylation of these intermediates under conditions of increased fluidity is not significantly different to the vecRK13 control cells. Lowering the cellular temperature decreases membrane fluidity and the addition of DMSO allows phase transition of membranes (into the gel phase) to occur at 25 ºC, resulting in reduced mobility of membrane proteins. No clear trends in signaling were observed for the 25 ºC (without DMSO) condition across the cell lines, either with or without exogenous copper (Supplementary information, Figure S4). The addition of DMSO increased the huRK13 phosphorylation of p38 and JNK/SAPK in the presence of copper but only the p38 phosphorylation is significantly raised when compared with the vecRK13 control. Thus, under conditions of reduced protein mobility due to gel phase transition of cellular membranes, huPrP is still able to elicit a PrP^C-specific response to copper through p38 signaling (Supplementary information, Figure S4). As observed previously ERK1/2 phosphorylation appeared to be a non-specific response to gel phase promoting conditions, with the vector control cells responding equivalently to the PrP^C-expressing cells (Supplementary information, Figure S3C).

Lipid raft disruption has a pronounced effect on moPrP-induced signal transduction in the presence of copper

The filipin III complex is an antibiotic that acts by binding and sequestering cholesterol. This makes it an efficient disruptor of lipid raft (cholesterol rich) membrane domains. The filipin treatment caused a non-specific increase of signal protein phosphorylation in all of the cell lines (Figure 4A-4C). When the cells were treated with filipin and copper together, the moRK13 cells showed a dramatic and significant increase in phosphorylation of all the three signal transduction proteins.

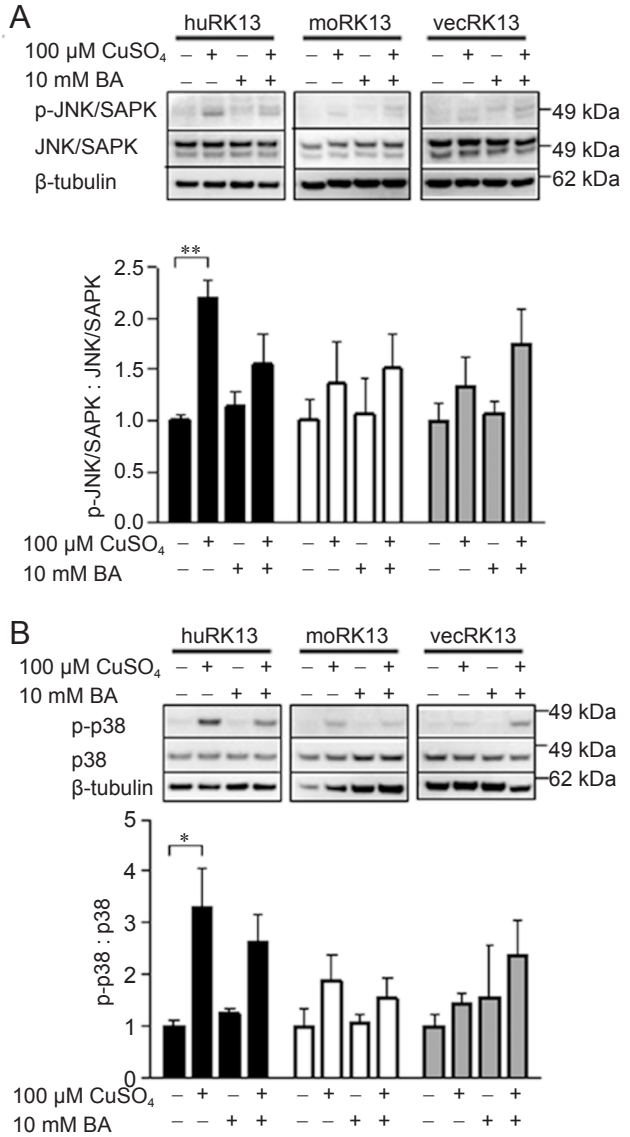

Figure 3 JNK/SAPK, and p38 activation in huRK13 and moRK13 cells exposed to increased exogenous copper and benzyl alcohol. HuRK13, moRK13 and vecRK13 cells were treated with increased exogenous copper for 30 min, both in the presence and absence of the membrane fluidizing agent benzyl alcohol. Lysates were western blotted with antibody sets against p-JNK/SAPK and JNK/SAPK **(A)**, p-p38 and p38 **(B)**. Bands were quantified densitometrically and huRK13, moRK13 and vecRK13 cells are shown as black, white and gray bars, respectively. Graphs represent the mean and s.e.m. (from four independent experiments) of the phosphorylated form to the total signaling protein ratio, and are expressed relative to the untreated cell control. Example blots are shown above the corresponding graph. Conditions that significantly changed the ratio of phospho-signaling molecule to signaling molecule, compared by one-way ANOVA within each cell line and by two-way ANOVA with the vecRK13 cell controls, are indicated by $*P < 0.05$, $**P < 0.01$ and $***P < 0.001$. Copper induces a huPrP-specific increase in JNK/SAPK and p38 phosphorylation, the specificity of which is lost when the membrane fluidity is increased.

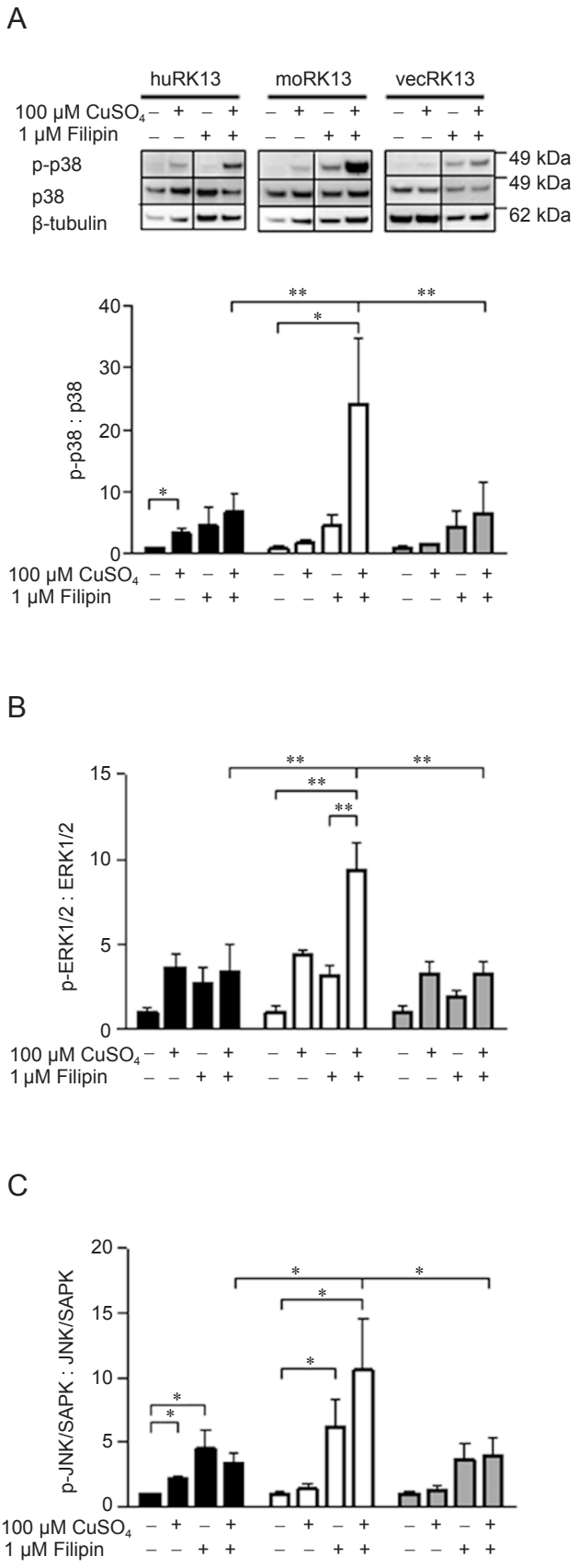

Activation of signal transduction in response to copper and filipin is dependent on the presence of moPrP

To check that the dramatic cellular signaling responses seen in response to the copper and filipin treatments were not due to clonal drift from selection pressure, the RNAi system described in Daude *et al*. [39] was employed to knock down the expression of PrP^C in the moRK13 cells, and by doing so to allow the innate responses of the cell line to be assessed in the setting of attenuated PrP^C expression. ERK1/2 signaling was assessed in the knockdown cells following treatment with copper and filipin. ERK1/2 signaling was chosen for analysis because ERK1/2 phosphorylation was altered in these cells basally and, whilst ERK1/2 responses to copper alone were non-specific, significant increases were observed in the moRK13 cells when the copper was applied with filipin. Further, Daude *et al*. [39] used ERK as a loading control, so we were confident that ERK1/2 levels would not be altered by the siRNA transfection. Since the moRK13 cells are transfected to overexpress PrP^C, a complete knockdown of PrP proved difficult; however a ~30% reduction in protein expression was reproducibly achieved (Figure 5A and 5B), and this corresponded with a ~48% decrease in ERK1/2 phosphorylation when treated with copper and filipin (Figure 5A and 5C) compared with cells expressing unaltered levels of moPrP. Therefore, it is unlikely that the cell line has suffered clonal drift that would account for the signaling responses. Instead $moPrP^C$ seems essential for these signaling responses to occur. To further ensure that the cell lines used had not drifted from the original population, the untransfected RK13 cells were treated with the copper and filipin con-

Figure 4 Induction of signal transduction in huRK13, moRK13 and vecRK13 cells by copper when lipid rafts are disrupted. The cholesterol-sequestering antibiotic filipin was used to increase membrane fluidity by disrupting the cholesterol-rich lipid raft domains and cells were treated for 30 min with and without copper before lysis and western blotting. Example blots of p38 activation† are shown above the corresponding graphical data in **(A)** and graphical data only for ERK and JNK/SAPK are shown in **(B)** and **(C)**, respectively. Graphs represent the mean and s.e.m. of four independent experiments of huRK13 (black bars), moRK13 (white bars) and vecRK13 (gray bars) cells. MoRK13 cells show a dramatic and significant response (in contrast to hu/vecRK13 cells) of all of the signaling proteins to the filipin and copper treatment (ERK, F = 12.86, $P < 0.0001$; p38, F = 3.506, $P = 0.0494$; JNK/SAPK, F = 7.663, $P = 0.0003$; $*P < 0.05$, $**P < 0.01$, $***P < 0.001$). †These blots are separated between the filipin and non-filipin treatments, as these conditions were originally run on the same blot (for quantification purposes) with bands for other treatments between the two conditions; these have been removed to show only the relevant data here.

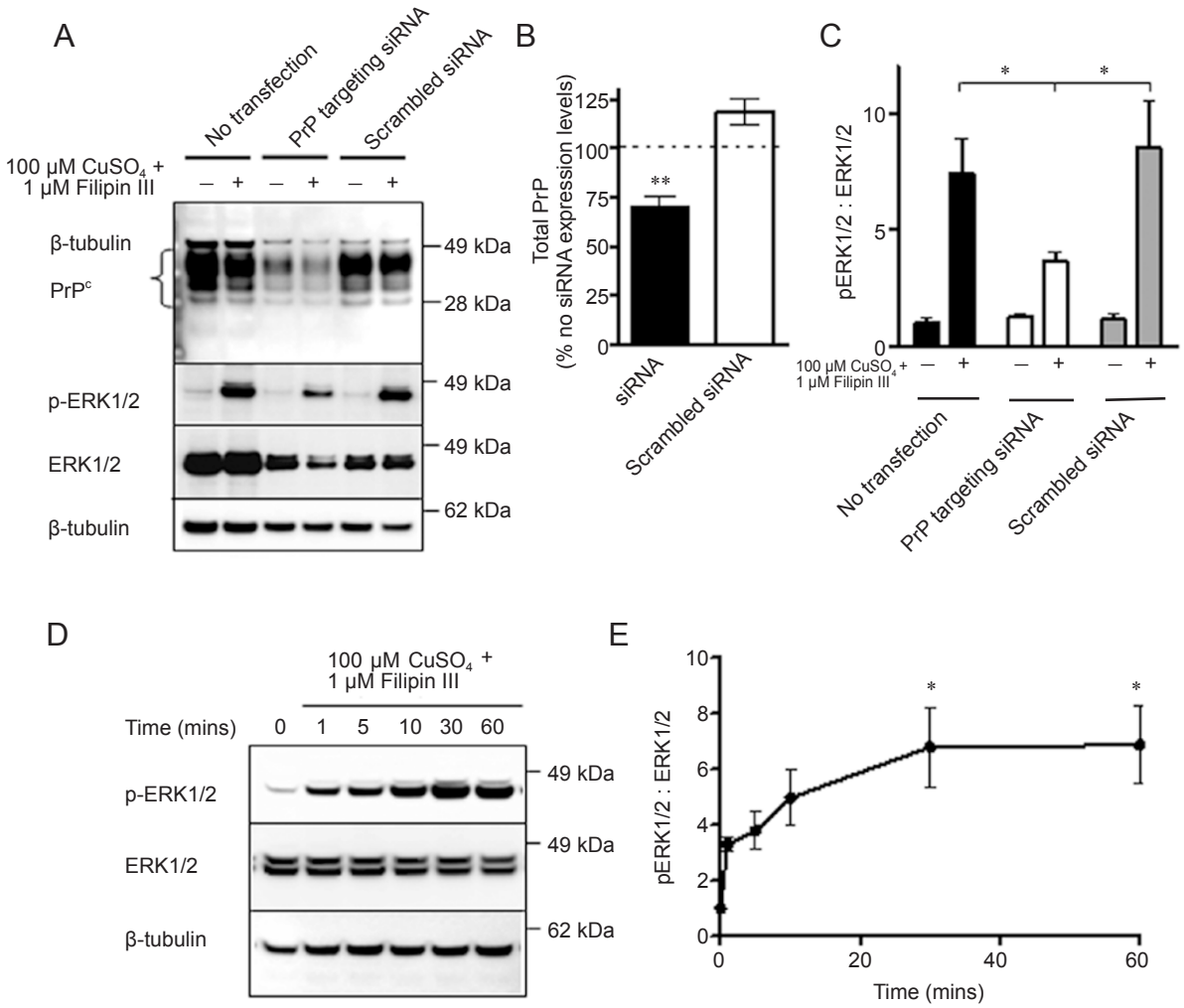

Figure 5 Dependence on moPrP^C expression and time frame of the copper- and filipin-mediated signal transduction event. **(A**-**C)** RNAi knockdown of the overexpressing moRK13 cell line was carried out using transient transfection of siRNA duplexes targeted against PrP^C or scrambled as a control for non-specific responses to transfection. **(A)** Western blots of PrP and ERK1/2 signaling in the untransfected, siRNA-transfected cells and scrambled siRNA controls, when treated with and without 100 μM copper and 1 μM filipin III. **(B)** Densitometric quantification of the PrP^C western blots. Expression of PrP^C is significantly reduced in the cells receiving the siRNA directed against PrP^C (black bar; $t = 5.549$, $P = 0.0051$, $n = 3$) but not in those receiving the scrambled siRNA (white bar; $t = 2.81$, $P = 0.107$, $n = 3$). **(C)** Induction of ERK1/2 signaling, shown as the ratio of p-ERK1/2 to total ERK1/2, by 100 μM copper and 1 μM filipin III is reduced in cells transfected with siRNA directed against PrP^C ($F = 40.23$, $P < 0.0001$, $n = 3$, $^*P < 0.05$; black, white and gray bars represent no siRNA, PrP-targeting siRNA and scrambled control siRNA, respectively). **(D**, **E)** Activation of ERK1/2 when moRK13 cells were treated with 100 μM copper and 1 μM filipin III was followed over a period of 1 min to 1 h. Blots are shown in the left plate **(D)** and densitometric quantification of the p-ERK1/2 to total ERK1/2 ratio in the right panel **(E)**. Phosphorylation of ERK1/2 is seen from immediately post treatment and plateaus after 10 min of treatment. Statistical significance is achieved at 30 min and maintained until 60 min ($F = 4.831$, $P = 0.0165$, $n = 4$, $^*P < 0.05$). Graphs show the mean and s.e.m..

ditions. The results obtained were not significantly different from the vecRK13 cells (Supplementary information, Figure S5).

Copper- and filipin-induced signal transduction occurs rapidly and peaks around 30 min after exposure

To make certain that the 30 min time point at which the various treatments were assessed was not limiting the responses seen, especially as many ERK1/2 signal transduction events occur within minutes of stimuli, a time course was performed on the moRK13 cells. Cells were treated with the copper and filipin treatments from 1-60

min and western blotted for ERK1/2 phosphorylation. Activation of signaling can be seen as early as 1 min post exposure to copper and filipin, and phosphorylation continues to increase until 30 min, after which it appears to start decaying (Figure 5D and 5E). Significant difference is achieved at the 30 and 60 min time points.

Cell lines endogenously expressing PrP^C show similar profiles to the transfected RK13 cell lines

Whilst PrP^C transfection into a neutral host species provides a convenient background for looking at protein sequence-specific responses, the behavior of endogenously expressed proteins may still vary. The human SH-SY5Y and mouse Neuro2a (N2a) cell lines were used to look at the responses of cells endogenously expressing PrP, and the mouse PrP-null CF10 cell line [40] was additionally considered to identify PrP-specific responses. These cell lines are derived from neuronal lineages, whereas the RK13 cells are epithelial, and would, therefore, identify distinct reactions observed due to cell origin differences. Each of the cell lines were assayed with the copper and filipin conditions as described for the RK13 cell lines and western blotted for ERK1/2 (Figure 6A), p38 (Figure 6B) and JNK/SAPK (Figure 6C), and the SH-SY5Y and N2a cells were additionally western blotted for PrP following PNGase F digesting (Figure 6D). The signaling trends seen in the RK13 cells are mostly preserved across the cell lines, with the mouse N2a cells showing significant increases in phosphorylation of all signal transduction intermediates in response to the combined copper and filipin condition. The human SH-SY5Y cells, whilst retaining the reduced phosphorylation response to copper and filipin, do not show the increase in phosphorylation of p38 and JNK/SAPK in response to copper alone that was seen for the huRK13 cells. This may indicate that the copper-induced signaling by huPrP when lipid raft integrity is preserved is influenced by cell lineage or that overexpression of huPrP in the RK13 background renders it more poised to respond to copper than when expressed at endogenous levels. The cleavage profiles are not identical to those seen in the RK13 cells, with the SH-SY5Y cells showing very limited cleavage responses but the N2a cells showing a significant increase in N1/C1 cleavage in response to combined copper and filipin treatment.

Introduction of the human N1/C1 cleavage region motif into mouse PrP^C results in mixed cleavage and signaling responses

The region encompassing the human N1/C1 cleavage site has two methionines, which are lacking in the mouse sequence (Supplementary information, Figure S1A, boxed); this is known as the 3F4 site, as this sequence is detected by the 3F4 anti-PrP antibody. To further investigate how the N1/C1 cleavage site influences the mouse PrP^C response to increased exogenous copper and the membrane-perturbing conditions, this motif was cloned into the mouse sequence and stable mixed population cell lines were selected, referred to as 3F4moRK13 cells. Basally, 3F4moRK13 cells showed less N1/C1 cleavage than moRK13 but more than huRK13 cells (Figure 7A and 7B), and N1/C1 cleavage in 3F4moRK13 cells was not significantly affected by copper and/or filipin treatment (Figure 7C). No significant difference in the basal levels of the C2 fragment was observed (data not shown). A basal difference is also apparent for ERK1/2 phosphorylation, with 3F4moRK13 showing decreased levels of phosphoERK1/2 compared to huRK13 but greater levels than moRK13 cells (Figure 7D and 7E). The N1/C1 cleavage correlates inversely with the basal phosphorylation levels ($r^2 = 0.88$, $P < 0.0001$). The 3F4moRK13 cells were treated with copper and/or filipin in parallel with the mixed population moRK13 and huRK13 cells as described previously. The PrP^C-independent response of ERK1/2 phosphorylation to copper treatment was maintained in the 3F4moRK13 cells (Figure 7D and 7F); conversely, the specific response of the moRK13 cells to the combined filipin and copper treatment was lost, with the 3F4moRK13 cells showing no significant difference from the huRK13 cell response. The huRK13-specific phosphorylation of p38 and JNK/SAPK in response to copper was also abolished (Figure 7G-7I), and all phosphorylation appeared reduced. The consistency of the cellular responses did, however, show that, although attenuated, the increase in JNK/SAPK phosphorylation that was observed for moRK13 cells after treatment with both filipin and copper was still significant for the 3F4moRK13 cells, but this was not the case for p38 phosphorylation.

Discussion

Our results suggest PrP^C alpha cleavage and PrP^C-mediated signal transduction may be linked events. Further, both events are influenced by cell membrane and particularly lipid raft integrity. In the context of the neutral RK13 cell background, the primary sequence of PrP^C, specifically the N1/C1 cleavage site, exerts a dominant influence over signal transduction through MAPK intermediates both basally and in response to membrane perturbation in the presence of copper. These effects are summarized in Figure 8.

In the current study, increased basal N1/C1 cleavage was associated with lower basal ERK phosphorylation, but increased N1/C1 cleavage in response to perturbation

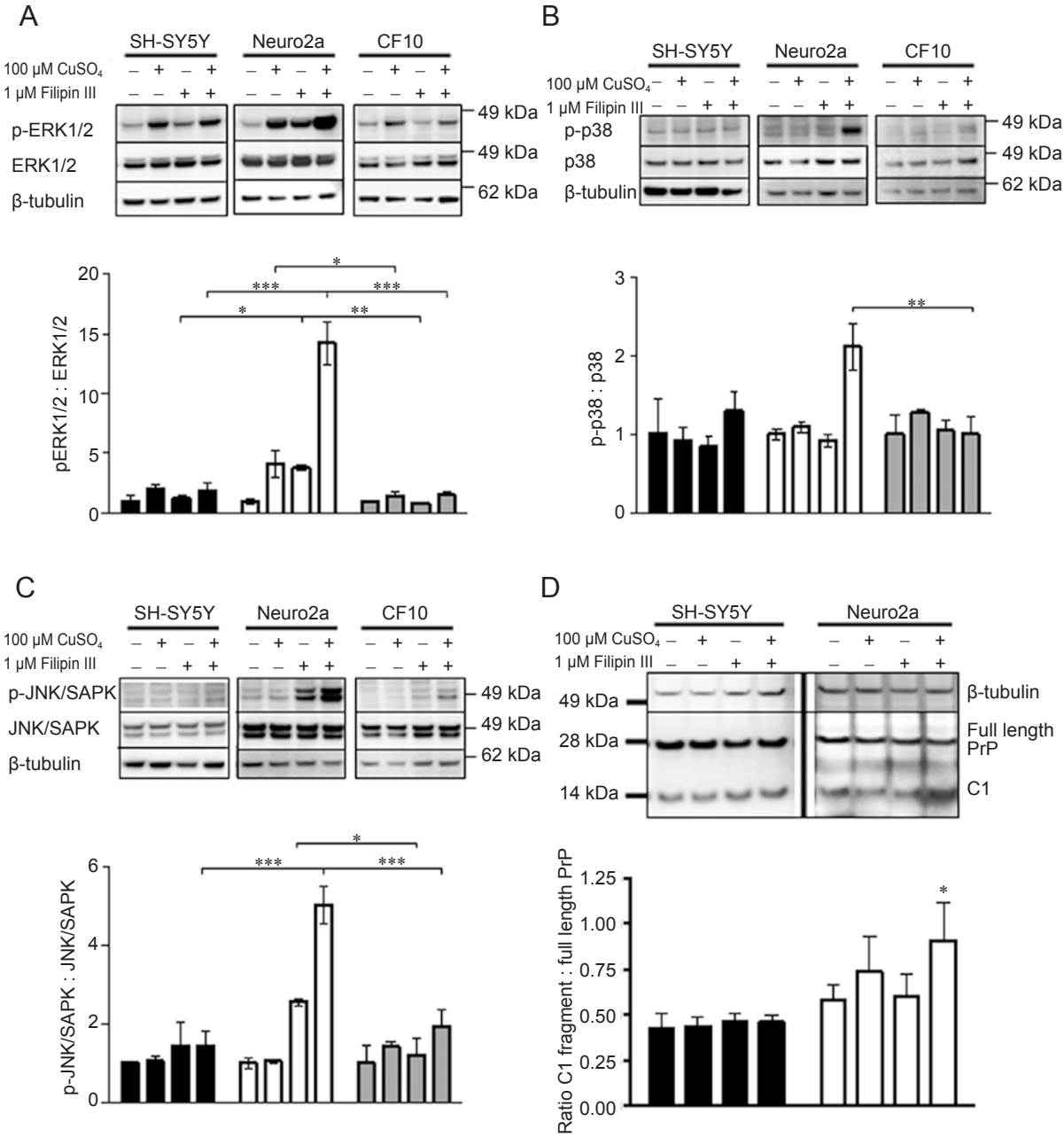

Figure 6 Human SH-SY5Y and murine Neuro2a cell responses to copper and filipin treatments. To consider how the 100 μM copper and 1 μM filipin III treatments may alter signaling and cleavage in cell lines endogenously expressing PrP^C, and, hence not subject to overexpression or selection pressure artifacts, the aforementioned treatments were carried out on SH-SY5Y and Neuro2a (N2a) cell lines as described for the RK13 cell lines. The murine neuronal PrP-null CF10 cell line was also compared to look for PrP-specific responses. **(A-C)** Western blot and densitometric quantification (mean and s.e.m.) of SH-SY5Y (black bars), N2a (white bars) and CF10 (gray bars) cells treated with copper, filipin, or copper and filipin together to disrupt lipid rafts. Shown are the changes in ERK1/2 **(A)**, p38 **(B)** and JNK/SAPK **(C)** signal transduction as ratios of the phosphorylated form of the signal protein to the total expression levels and normalized to untreated cells. Significant differences, as determined by two-way ANOVA with Bonferroni secondary testing, were seen between the N2a and both the SH-SY5Y and CF10 cell lines (ERK1/2 F = 67.39, $P < 0.0001$, $n = 4$; p38 F = 3.96, $P = 0.018$, $n = 4$; JNK/SAPK F = 12.50, $P = 0.0001$, $n = 4$; $^*P < 0.05$, $^{**}P < 0.01$, $^{***}P < 0.001$). **(D)** PrP N1/C1 cleavage of SH-SY5Y (black bars) and N2a (white bars) cells following treatment with copper, filipin, and copper with filipin. Shown are western blot of the PNGase F-treated cell lysates and densitometric quantification of band intensities. Two-way ANOVA with Bonferroni secondary testing identifies that the cell lines are significantly different from each other (F = 9.314, $P = 0.0055$, $n = 4$, $^*P < 0.05$).

resulted in increased signal transduction through MAPK intermediates. This may indicate that N1/C1 processing preceded PrP^C localization at the cell surface, and that sequestration of the cleavage fragments in lipid raft domains renders them inactive. Release from the lipid raft domains by cholesterol depletion or other cellular perturbations may allow rapid activation of signal transduction pathways in response to stimuli such as copper. Raft sequestration is a known control mechanism for the activation/deactivation of certain enzymes. An example of this is TACE, where raft sequestering suppresses its catalytic activity until released [41]. Alternatively, release from rafts may allow TACE to cleave PrP at the N1/C1 site and once a threshold is reached the N1/C1 cleavage fragments produce dramatic cellular response. The former suggestion is supported by a recent study from Walmsley *et al*. [42], where alpha cleavage appears to occur along the secretory pathway, probably in the Golgi, on the way to the cell surface. The increase in PrP^C N1/C1 cleavage may, therefore, follow the signal transduction event to replenish PrP^C C1 at the cell surface. The activation of signal transduction intermediates by human PrP^C where no response was seen for mouse PrP^C, despite the higher basal levels of alpha cleavage, may reflect differing abilities of the two proteins to engage the signal transduction machinery.

The 3F4 epitope alters the structure of the alpha cleavage site as shown by the recognition specificity of the 3F4 antibody. The sulfur-containing methionines, as found in the human sequence, are substantially different from the charged histidine with its imidazole ring and the small aliphatic valine of the mouse sequence. *PRNP* point mutations within the structured C-terminal region are associated with human prion diseases, therefore supporting the likelihood that introduction of the 3F4 epitope into murine *PRNP* may have significant biological consequences. The difference in sequence may result in a different presentation of the alpha cleavage site to processing enzymes, resulting in the observed different cleavage patterns, which in turn influences PrP^C function. These potential downstream biological consequences of this sequence variation may impact on studies that use the 3F4 epitope to differentiate between human and mouse PrP^C when overexpressing one in the cellular background of the other. Researchers using these constructs in the future may wish to consider the bearing this may have on conclusions about the function of PrP^C.

N1/C1 cleavage is partially under the control of ADAM10 and TACE activities [28]. Unlike ADAM10, TACE has a very narrow substrate specificity [43]; TNFα, its preferred substrate, is cleaved between alanine and valine residues as found at the mouse N1/C1 cleavage site but not at the human. TACE may therefore have a greater role in the N1/C1 cleavage of mouse PrP^C than human, particularly under altered cellular conditions. The intermediate extent of the N1/C1 cleavage of the 3F4moRK13 cells also indicates that, whilst the N1/C1 site is clearly influencing this cleavage, further sequence differences appear to be involved, perhaps by modulating binding partner interfaces, membrane interaction or cellular trafficking.

Regardless of primary sequence, copper loading appeared to play an important role in PrP^C-mediated MAPK signal transduction. The activation of signal transduction in the moRK13 cells following lipid raft disruption was not due to the potential toxicity of copper, since a lesser reaction was observed following copper treatment alone. Copper binding has been reported to be essential for PrP^C protection against oxidative stress [44, 45], and this protection may be via activation of signal transduction pathways and the subsequent cellular response [30]. Furthermore, there is recent evidence for MAPK activation by signaling endosomes [15]. PrP^C is internalized in response to copper [46], and this reaction requires the octameric repeat domain and the palindromic sequence starting at the N1/C1 cleavage site to be intact [47, 48]. Signaling endosomes have been especially associated with clathrin and dynamin mediated internalization [15, 49, 50], and these are both pathways with which PrP^C has been shown to interact [51, 52]; hence, the role of copper in these reactions may be to promote the internalization of PrP^C to facilitate engagement with signaling intermediates. This is further supported by the findings of Caetano *et al*. [53], who show that signaling by STI-1 through ERK1/2 requires internalization of PrP^C and was inhibited by a dominant-negative mutant of dynamin.

Although multiple binding partners for PrP^C have been suggested to have a role in the activation of cellular signal transduction, including Grb2, EGFR and caveolin [21, 23, 25], the part PrP^C processing plays in relation to such events is uncertain. N1/C1 cleavage has been shown to play a role in apoptosis through modulation of caspase-3 activation. The C1 fragment is able to increase p53 transcription and induce caspase-3 activation [54]. In transgenic mice overexpressing a truncated PrP species (lacking amino acids 32-134), caspase-3 activation is via ERK1/2 and p38 activation [55]. The finding that ERK1/2 and p38 signal protein activation correlated with the changes in mouse C1 cleavage suggests that the mouse PrP^C may be able to interact more efficiently or with a greater number of intermediates involved in activating these pathways. The human PrP^C-expressing cells demonstrated more restricted associations by showing a significant linkage only between N1/C1 cleavage and

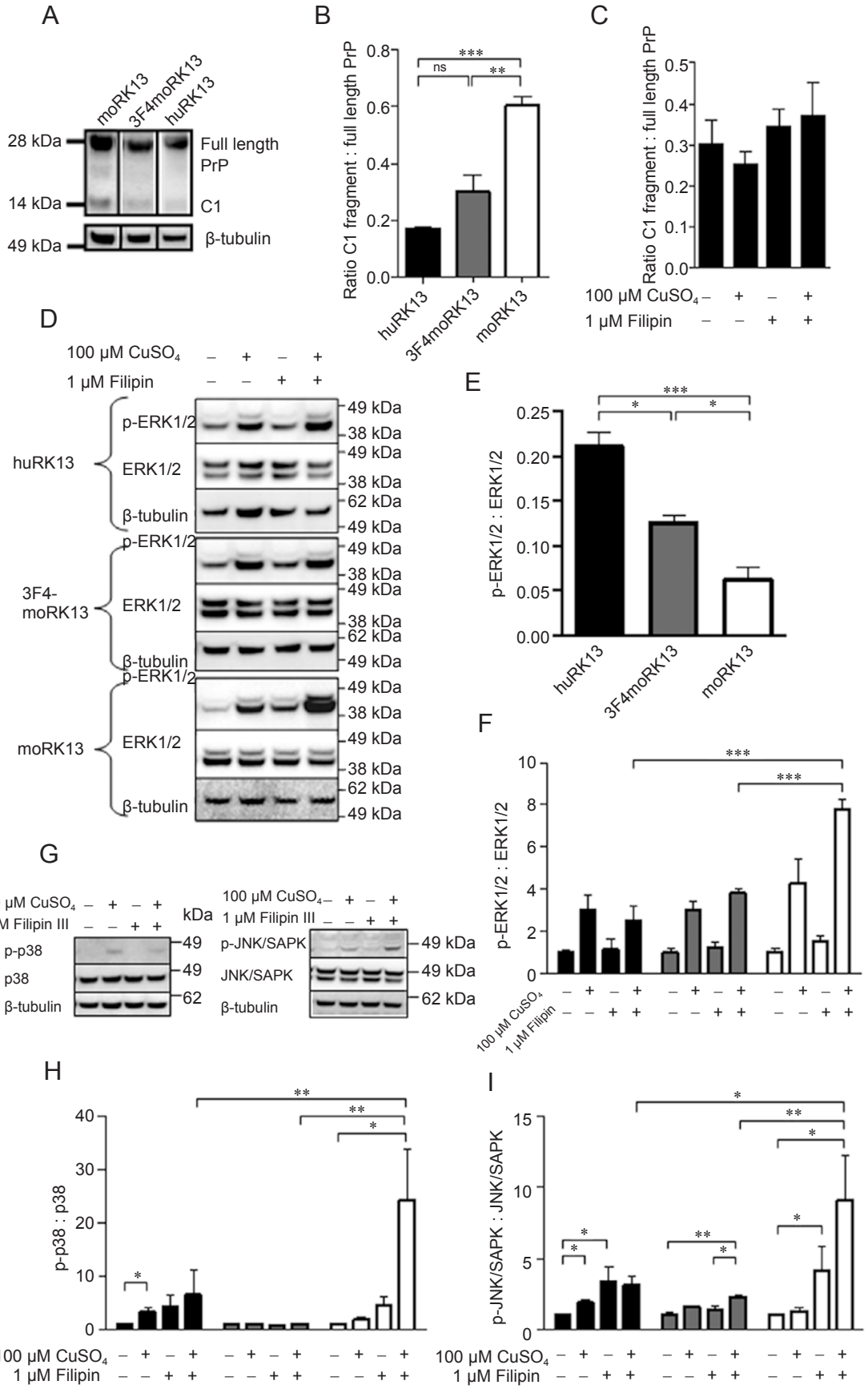
A
moRK13
3F4moRK13
huRK13
28 kDa
14 kDa
49 kDa
Full length PrP
C1
β-tubulin
B
Ratio C1 fragment : full length PrP
ns
**
***
huRK13
3F4moRK13
moRK13
C
Ratio C1 fragment : full length PrP
100 μM CuSO4
1 μM Filipin
D
100 μM CuSO4
1 μM Filipin
huRK13
3F4-moRK13
moRK13
p-ERK1/2
ERK1/2
β-tubulin
49 kDa
38 kDa
62 kDa
E
p-ERK1/2 : ERK1/2
*
***
F
p-ERK1/2 : ERK1/2
G
100 μM CuSO4
1 μM Filipin III
kDa
p-p38
p38
β-tubulin
p-JNK/SAPK
JNK/SAPK
H
p-p38 : p38
I
p-JNK/SAPK : JNK/SAPK

Figure 7 Introduction of the 3F4 epitope into moPrP alters cleavage and signaling profiles both basally and in response to copper and filipin treatments. Example PNGase-F-digested basal PrP blots **(A)** and densitometric quantification **(B)** of huRK13, moRK13 and 3F4moRK13 cells. C1 cleavage of the 3F4moPrP falls between the levels of moPrP and huPrP, and is significantly different from moPrP. Cells were treated with copper and the lipid-raft disrupting antibiotic filipin for 30 min. Alterations in PrP N1/C1 cleavage are shown in **(C)**. Example ERK1/2 blots are shown in **(D)**. Densitometric quantification of this data show that basal ERK1/2 phosphorylation differs across the cell lines with the 3F4moRK13 levels greater than the moRK13 but lower than the huRK13 cells, and statistically different to both **(E)** ($F = 29.86$, $P = 0.0002$, $n = 4$). The ability of 3F4moRK13 cells to induce ERK1/2 signaling in response to the filipin and copper treatment is significantly reduced compared to moRK13 cells **(F)** ($F = 34.83$, $P < 0.0001$). p38 (blots are shown in **G** and quantification in **H**) and JNK/SAPK (blots are shown in **G** and quantification in **I**) signaling of the 3F4moRK13 cells are significantly different from both huRK13 and moRK13 cells(p38, $F = 3.385$, $P = 0.0284$, $n = 3$; JNK/SAPK, $F = 3.805$, $P = 0.0142$, $n = 3$), with the 3F4moRK13 cells showing a lesser ability to signal through these molecules; however, JNK/SAPK phosphorylation is still significantly increased above untreated cells in response to filipin and copper together ($F = 9.376$, $P = 0.0054$, $n = 3$; $^{*}P < 0.05$, $^{**}P < 0.01$, $^{***}P < 0.001$). All plots represent the mean and s.e.m. of four independent experiments and black, grays and white bars represent the huRK13, 3F4moRK13 and moRK13 cell line results, respectively.

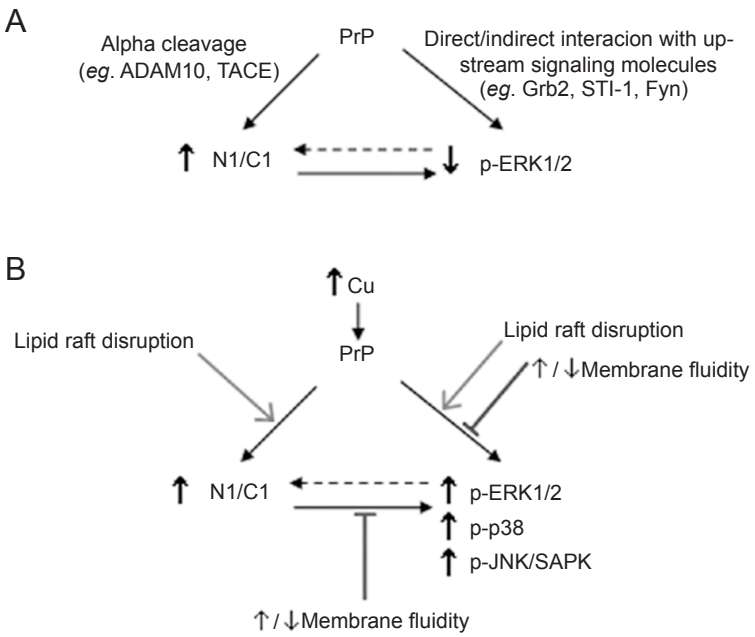

Figure 8 Schematic depiction of PrP N1/C1 cleavage and MAPK-signaling relationships. **(A)** The relationship between PrP N1/C1 cleavage and ERK1/2 phosphorylation in the RK13 cells in the unperturbed state, showing the inverse relationship. **(B)** The relationship between the PrP cleavage and intracellular signaling when an increased amount of exogenous copper is available to PrP. In the presence of copper, a direct relationship is observed between N1/C1 cleavage and signaling. Open arrowheads show how lipid raft disruption enhances these effects and blocked arrows indicate how non-specific changes in fluidity alter the specificity of the reactions.

p38 activation. The consistency of the PrP^{C} signal across the western blots also shows that the alteration in signaling is not due to significant amounts of PrP^{C} dissociating from the cell surface due to shedding of the GPI anchor, as has previously been reported in response to filipin and copper [56, 57]. This could be due to species or cell culture model differences. Rabbit PrP^{C} varies from human and mouse PrP^{C} around the site of the GPI anchor; consequently, the rabbit host enzymes involved in cleavage at the GPI anchor may have a lower recognition for human and mouse PrP^{C}, resulting in less shedding within this system.

The N2/C2 cleavage event was also considered during this study (Supplementary information, Figure S6); however, alterations in N2/C2 cleavage did not correlate with any PrP-related selective change in the MAPK-signaling

intermediates studied. Overall, there was no difference between moRK13, huRK13 or 3F4moRK13 basal N2/C2 processing. This is to be expected if the primary cleavage mechanism at the N2/C2 cleavage site is ROS-related, as there was no difference in intracellular ROS production between the cell lines, nor in the N2/C2 site motifs of human and mouse PrP^C. Moreover, it shows that the N1/C1 cleavage has no direct influence on the N2/C2 cleavage.

Transfecting different PrP primary sequences into identical host cells with negligible endogenous expression allowed focused research and detection of potential species-related differences in processing, particularly at the alpha site, and consequent activation of MAPK signaling. Further studies are required to confirm that the associations we found between PrP^C processing and activation of MAPK signaling are mechanistically directly linked steps in a cellular pathway, rather than simply occurring as unrelated parallel events. Further, while the RK13 cells afforded a permissive and conveniently manipulable system for the expression of PrP constructs of interest, the applicability and translation of our findings from these overexpressing cells of epithelial origin to the situation occurring in neuronal cells endogenously expressing PrP^C is supported by data with SH-SY5Y and N2a cell lines.

In conclusion, the data presented here relate PrP^C processing to signal transduction, and show the inter-dependence of the PrP^C primary sequence, particularly the N1/C1 cleavage site, and the cell membrane in these events. The PrP^C primary sequence influences the predominant type of proteolysis likely to occur in response to specific cellular perturbations, and to what extent consequent signal transduction will occur. Generally, membrane integrity appears important for the fidelity of signal transduction occurring in relation to PrP^C processing, although under certain conditions membrane disruption may allow proteolytic processing not normally accessible to the particular PrP^C primary sequence. For huRK13 cells, the selectivity of signal transduction activation due to copper treatment was often lost when membrane integrity was compromised, becoming similar to non-PrP^C-expressing cells. Independent of the overall PrP^C primary sequence, increased N1/C1 cleavage of PrP^C appears linked to the MAPK pathway, with alterations in amino acid sequence at this proteolytic site markedly influencing processing and signal transduction.

Materials and Methods

Cell culture

All cell lines were cultured in Dulbecco's Modified Eagles Media (DMEM; Gibco – Invitrogen, Victoria, Australia) supplemented with 10% fetal bovine serum (Invitrogen), 50 U/ml penicillin and 50 μg/ml streptomycin solution (Sigma-Aldrich; New South Wales, Australia). Cells were maintained at 37 ºC with 5% CO_2 in a humidified incubator. For microtitre plate assays, (used unless otherwise stated) cells were plated to be 90%-95% confluent at the start of the assay.

Constructs and transfection

pIRES-puro2 (Clontech – Scientifix, Victoria, Australia) contain the full-length human or mouse PrP^C open reading frame, as well as the vector alone was transfected into RK13 cells using FuGene 6 transfection reagent (Roche, New South Wales, Australia) as per the product protocol for a 3:1 reagent:DNA ratio. A total of 2.5 μg/ml puromycin (Sigma-Aldrich) was used for cell selection and both stable clones of equivalent expression levels and mixed populations were selected. Cells were maintained in 2.5 μg/ml puromycin during routine culture. A further mixed population cell line expressing moPrP with the 3F4 epitope (human N1/C1 cleavage site motif) was created by transfection using Lipofectamine (as per the product protocol: Invitrogen). The mixed population was selected and maintained as described above.

RNAi

The siRNA duplexes described by Daude *et al*. [39] were purchased from Sigma-Aldrich. Cells were plated 1 day prior to treatment with the siRNA at approximately 50% confluence. siRNA duplexes were delivered into the cells using FuGene HD transfection reagent in a 4:1 reagent:siRNA ratio as described in the product protocol. The final concentration of duplexes delivered to the cells was 400 nM. Cells were then incubated for 2 days under standard conditions before treatment and extraction as described below.

Western blot

Cells were treated for 30 min with appropriate test reagent before lysis in 20 μl RIPA buffer (50 mM Tris-HCl pH 7.4, 150 mM NaCl, 0.1% (w/v) SDS, 0.5% (w/v) sodium deoxycholate, 1% (v/v) NP-40) supplemented with 0.5 U/ml Benzonase (Sigma-Aldrich) for 20 min at 37 °C. Lysates were mixed with 10 μl of 3× LDS loading dye (Invitrogen) supplemented with 5% (v/v) β-mercaptoethanol (Sigma-Aldrich) and denatured gently at 80 °C for 10 min. A total of 20 μl of lysate was loaded into 15-well 12% NuPAGE Bis-Tris gels (Invitrogen). Gels were run at 200 V for 35-40 min (until the dye front reached the bottom) in the Invitrogen NuPAGE gel tank system, using MES running buffer (Invitrogen). Gels were transferred onto a nitrocellulose membrane (BioRad, New South Wales, Australia) in a Bio-Rad wet blotting system at 100V for 45 min. Membranes were blocked for 1 h in 5% (w/v) fat-free milk powder in PBS-0.1% (v/v) Tween-20 (PBS-t). For PrP^C detection, western blot incubations used a 1 in 30 000 ICSM-18 primary monoclonal antibody (mab; mouse epitope 142-152, human epitope 143-153 (DGen, London, UK)) in 1% milk PBS-t; with anti-mouse HRP secondary (GE Healthcare, New South Wales, Australia). Signaling antibodies phospho(T202/Y204)-p44/42 (p44/42 is more commonly known as ERK1/2, therefore, p-ERK1/2 is used to refer to this antibody); p44/42 (ERK1/2); phospho(T180/Y182)-p38 (p-p38); p38; phospho(T183/Y185)-JNK/SAPK (p-JNK/SAPK); and SAPK/JNK were all used at 1 in 1 000 dilution (Cell Signaling – Genesearch Pty, Queensland, Australia) in 1% (w/v) bovine serum albumin (BSA; Sigma-Aldrich)

in PBS-t, with 1 in 5 000 anti-rabbit HRP secondary (Cell Signaling) in 1% (w/v) BSA in PBS-t. Anti-β-tubulin (Sigma-Aldrich) was used as a loading control and blotted using a 1 in 20 000 dilution with anti-mouse-HRP secondary used at 1 in 10 000. Membranes were stripped between probing with each antibody by incubation in low-pH stripping buffer (25 mM glycine-HCL, pH 2; 1% (w/v) SDS) for 10 min at room temperature with agitation, and then washed once in PBS-t before incubation in blocking solution for 1 h.

PNGase F digestion

Media were removed from the cells and 20 µl RIPA buffer plus 0.5 U/ml Benzonase were added per well. Plates were incubated at 37 °C for 20 min. A total of 2 µl 10× denaturation buffer (5% (w/v) SDS, 5% (v/v) β-mercaptoethanol, 50 mM EDTA, 0.02% (v/v) sodium azide in PBS, pH 8.0) was added per well and samples were heated at 80 °C for 10 min to denature. The plate was allowed to cool to room temperature, and 2.5 µl 10% (v/v) NP-40 and 5.5 µl incubation buffer (50 mM EDTA and 0.02% (v/v) sodium azide in PBS, pH8.0) plus 1 U PNGase F (Sigma-Aldrich) were added per well. Plates were incubated overnight at 37 °C in a humidified chamber. 3× NuPAGE LDS sample loading buffer supplemented with 5% (v/v) β-mercaptoethanol was added to the wells and samples were denatured at 80 °C for 10 min. A total of 20 µl of sample was loaded per well, with PrP^C detection as described above.

DCFDA assay

Media were removed and replaced with 50 µl of dPBS containing 5 µM 5-(and-6)-chloromethyl-2',7'-dichlorodihydrofluorescein diacetate, acetyl ester (CM-H_2-DCFDA, Invitrogen). Cells were incubated at 37 °C for 20 min, then the probe solution was removed and replaced with 100 µl of Opti-MEM® I Reduced-Serum Medium (without phenol red) with or without test reagent added. Readings were taken at time 0 and 30 min, using 488 nm excitation and 530 nm emission filters in a Fluostar Optima (BMG Labtech, Victoria, Australia).

Densitometry and statistical analyses

Luminescent signal of the bands on the western blots was captured using a Las-3000 intelligent darkbox (FujiFilm – Berthold, Victoria, Australia), and the intensity was quantified after the subtraction of background, by ImageJ 1.38×. Statistical analyses were carried out using GraphPad Prism 4 or Minitab15 statistical software. Two-way ANOVA with Bonferroni secondary tests was used to determine different cell line responses to the same conditions (these are tabulated in Supplementary information, Table S1) and one-way ANOVA with Tukey's secondary test was used to identify differences within a single cell line. The graphs shown throughout show the mean ± s.e.m. of all of the data; blots from replicate clone/mixed cell line data were averaged and treated as one repeat.

Acknowledgments

CF10 cells were a kind gift from Dr Suzette Priola (National Institutes of Health, USA). The authors thank Ms Robyn Sharples (The University of Melbourne, Australia) for technical assistance. This work was supported by an NH&MRC Program Grant (400202). CLH is supported by a University of Melbourne Early Career Researcher Grant; SJC by an NH&MRC Practitioner Fellowship (400183); SJC and VAL by an NH&MRC Project Grant (454546); VAL is supported by a University of Melbourne CR Roper Fellowship; VAL and AFH by an NH&MRC Project Grant (400229); and AFH by an NH&MRC Career Development Award (251745).

References

1 Prusiner SB. Novel proteinaceous infectious particles cause scrapie. *Science* 1982; **216**:136-144.
2 Legname G, Baskakov IV, Nguyen HO, *et al*. Synthetic mammalian prions. *Science* 2004; **305**:673-676.
3 Büeler H, Fischer M, Lang Y, *et al*. Normal development and behaviour of mice lacking the neuronal cell-surface PrP protein. *Nature* 1992; **356**:577-582.
4 Brandner S, Raeber A, Sailer A, *et al*. Normal host prion protein (PrP^C) is required for scrapie spread within the central nervous system. *Proc Natl Acad Sci USA* 1996; **93**:13148-13151.
5 Brown DR, Herms J, Kretzschmar HA. Mouse Cortical Cells lacking cellular PrP survive in culture with a neurotoxic PrP fragment. *Neuroreport* 1994; **5**:2057-2060.
6 Fischer M, Rulicke T, Raeber A, *et al*. Prion protein (PrP) with amino-proximal deletions restoring susceptibility of PrP knockout mice to scrapie. *EMBO J* 1996; **15**:1255-1264.
7 Chesebro B, Trifilo M, Race R, *et al*. Anchorless prion protein results in infectious amyloid disease without clinical scrapie. *Science* 2005; **308**:1435-1439.
8 Mallucci G, Dickinson A, Linehan J, Klöhn PC, Brandner S, Collinge J. Depleting neuronal PrP in prion infection prevents disease and reverses spongiosis. *Science* 2003; **302**:871-874.
9 Weissmann C, Büeler H, Fischer M, *et al*. PrP-deficient mice are resistant to scrapie. *Ann N Y Acad Sci* 1994; **724**:235-240.
10 Brown DR, Qin K, Herms JW, *et al*. The cellular prion protein binds copper *in vivo*. *Nature* 1997; **390**:684-687.
11 Hasnain SS, Murphy LM, Strange RW, *et al*. XAFS Study of the High-affinity Copper-binding Site of Human PrP^{91-231} and its Low-resolution Structure in Solution. *J Mol Biol* 2001; **311**:467-473.
12 Hornshaw MP, McDermott JR, Candy JM. Copper binding to the N-terminal tandem repeat regions of mammalian and avian prion protein. *Biochem Biophys Res Commun* 1995; **207**:621-629.
13 Jackson GS, Murray I, Hosszu LLP, *et al*. Location and properties of metal-binding sites on the human prion protein. *Proc Nat Acad Sci USA* 2001; **98**:8531-8535.
14. Allen JA, Halverson-Tamboli RA, Rasenick MM. Lipid raft microdomains and neurotransmitter signaling. *Nature Rev Neurosci* 2007; **8**:128-140.
15 Anderson DH. Role of lipids in the MAPK signaling pathway. *Prog Lipid Res* 2006; **45**:102-119.
16 Vigh L, Escribá PV, Sonnleitner A, *et al*. The significance of lipid composition for membrane activity: New concepts and ways of assessing function. *Prog Lipid Res* **44**:303-344.
17 Cashman NR, Loertscher R, Nalbantoglu J, *et al*. Cellular isoform of the scrapie agent protein participates in lymphocyte activation. *Cell* 1990; **61**:185-192.
18 Bainbridge J, Walker KB. The normal cellular form of prion protein modulates T cell responses. *Immunol Lett* 2005;

96:147-150.
19 Li R, Liu D, Zanusso G, *et al*. The expression and potential function of cellular prion protein in human lymphocytes. *Cell Immunl*. 2001; **207**:49-58.
20 Stuermer CA, Langhorst MF, Wiechers MF, *et al*. PrP^C capping in T cells promotes its association with the lipid raft proteins reggie-1 and reggie-2 and leads to signal transduction. *FASEB J* 2004; **18**:1731-1733.
21 Spielhaupter C, Schätzl HM. PrP^C directly interacts with proteins involved in signaling pathways. *J Biol Chem* 2001; **276**:44604-44612.
22 Lopes MH, Hajj GN, Muras AG, *et al*. Interaction of cellular prion and stress-inducible protein 1 promotes neuritogenesis and neuroprotection by distinct signaling pathways. *J Neurosci* 2005; **25**:11330-11339.
23 Monnet C, Gavard J, Mège RM, Sobel A. Clustering of cellular prion protein induces ERK1/2 and stathmin phosphorylation in GT1-7 neuronal cells. *FEBS Lett* 2004; **576**:114-118.
24 Schneider B, Mutel V, Pietri M, *et al*. NADPH oxidase and extracellular regulated kinases 1/2 are targets of prion protein signaling in neuronal and non-neuronal cells. *Proc Natl Acad Sci USA* 2003; **100**:13326-13331.
25 Toni M, Spisni E, Griffoni C, *et al*. Cellular prion protein and caveolin-1 interaction in a neuronal cell line precedes Fyn/ERK 1/2 signal transduction. *J Biomed Biotech* 2006; **2006**:1-13.
26 Mouillet-Richard S, Ermonval M, Chebassier C, *et al*. Signal transduction through prion protein. *Science* 2000; **289**:1925-1928.
27 Wopfner F, Weidenhöfer G, Schneider R, *et al*. Analysis of 27 mammalian and 9 avian PrPs reveals high conservation of flexible regions of the prion protein. *J Mol Bio* 1999; **289**:1163-1178.
28 Vincent B, Paitel E, Saftig P, *et al*. The Disintegrins ADAM10 and TACE contribute to the constitutive and phorbol ester-regulated normal cleavage of the cellular prion protein. *J Biol Chem* 2001; **276**:37743-37746.
29 McMahon HE, Mangé A, Nishida N, *et al*. Cleavage of the amino terminus of the prion protein by reactive oxygen species. *J Biol Chem* 2001; **276**:2286-2291.
30 Watt NT, Taylor DR, Gillott A, *et al*. Reactive oxygen species-mediated β-cleavage of the prion protein in the cellular response to oxidative stress. *J Biol Chem* 2005; **280**:35914-35921.
31 Chen SG, Teplow DB, Parchi P, *et al*. Truncated forms of the human prion protein in normal brain and in prion diseases. *J Biol Chem* 1995; **270**:19173-19180.
32 Yadavalli R, Guttmann RP, Seward T, *et al*. Calpain-dependent endoproteolytic cleavage of prpsc modulates scrapie prion propagation. *J Biol Chem* 2004; **279**:21948-21956.
33 Courageot MP, Daude N, Nonno R, *et al*. A cell line infectable by prion strains from different species. *J Gen Virol* 2008; **89**:341-347.
34 Vella LJ, Sharples RA, Lawson VA, *et al*. Packaging of prions into exosomes is associated with a novel pathway of PrP processing. *J Pathol* 2007; **211**:582-590.
35 Martin BD, Schoenhard JA, Sugden KD. Hypervalent chromium mimics reactive oxygen species as measured by the oxidant-sensitive dyes 2',7'-dichlorofluorescin and dihydrorhodamine. *Chem Res Toxicol* 1998; **11**:1402-1410.
36 Regev R, Assaraf YD, Eytan GD. Membrane fluidization by ether, other anaesthetics, and certain agents abolishes P-glycoprotein ATPase activity and modulates efflux from multidrug resistant cells. *Eur J Biochem* 1999; **259:**18-24.
37 Sangwan V, Örvar BL, Beyerly J, Hirt H, Dhindsa RS. Opposite changes in membrane fluidity mimic cold and heat stress activation of distinct plant MAP kinase pathways. *Plant J* 2002; **31**:629-638.
38 Shigapova N, Török Z, Balogh G, *et al*. Membrane fluidization triggers membrane remodelling which affects the thermotolerance in *Escherichia coli*. *Biochem Biophys Res Commun* 2005; **328**:1216-1223.
39 Daude N, Marella M, Chabry J. Specific inhibition of pathological prion protein accumulation by small interfering RNAs. *J Cell Sci* 2003; **116**:2775-2779
40 Greil CS, Vorberg IM, Ward AE, *et al*. Acute cellular uptake of abnormal prion protein is cell type and scrapie-strain independent. *Virology* 2008; **379**:284-293
41 Tellier E, Canault M, Rebsomen L, *et al*. The shedding activity of ADAM17 is sequestered in lipid rafts. Exp *Cell Res* 2006; **312**:3969-3980.
42 Walmsley AR, Watt NT, Taylor DR, Perera WS, Hooper NM. Alpha-cleavage of the prion protein occurs in a late compartment of the secretory pathway and is independent of lipid rafts. *Mol Cell Neurosci* 2009; **40**:242-248.
43 Mohan MJ, Seaton T, Mitchell J, *et al*. The tumour necrosis factor-α converting enzyme (TACE): A unique metalloproteinase with highly defined substrate specificity. *Biochemistry* 2002; **41**:9462-9469.
44 Brown DR, Clive C, Haswell SJ. Antioxidant activity related to copper binding of native prion protein. *J Neurochem*. 2001; **76**:69-76.
45 Haigh CL, Brown DR. Prion protein reduces both oxidative and non-oxidative copper toxicity. *J Neurochem* 2006; **98**:677-689.
46 Pauly PC, Harris DA. Copper stimulates endocytosis of the prion protein. *J Biol Chem* 1998; **273**:33107-33110.
47 Haigh CL, Edwards KE, Brown DR. Copper binding is the governing determinant of prion protein turnover. *Mol Cell Neurosci* 2005; **30**:186-196.
48 Perera S, Hooper NM. Ablation of the metal ion-induced endocytosis of the prion protein by disease associated mutation of the octarepeat region. *Curr Biol* 2001; **11**:519-523.
49 Howe CL, Valletta JS, Rusnak AS, Mobley WC. NGF signaling from clathrin-coated vesicles: Evidence that signaling endosomes serve as a platform for the Ras-MAPK pathway. *Neuron* 2001; **32**:801-814.
50 Sorkin A, Zastrow M. Signal transduction and endocytosis: close encounters of many kinds. *Nature Rev Mol Cell Biol* 2002; **3**:600-614.
51 Magalhães AC, Silva JA, Lee KS, *et al*. Endocytic intermediates involved with the intracellular trafficking of a fluorescent cellular prion protein. *J Biol Chem* 2002; **277**:33311-33318.
52 Shyng SL, Heuser JE, Harris DA. A glycolipid-anchored prion protein is endocytosed via clathrin coated pits. *J Cell Biol* 1994; **125**:1239-1250.
53 Caetano FA, Lopes MH, Hajj GN, *et al*. Endocytosis of prion protein is required for ERK1/2 signaling induced by stress-

inducible protein 1. *J Neurosci* 2008; **28**:6691-6702.
54 Sunyach C, Cisse MA, da Costa CA, Vincent B, Checler F. The C-terminal products of cellular prion protein processing, C1 and C2, exert distinct influence on p53-dependent staurosporine-induced caspase-3 activation. *J Biol Chem* 2007; **282**:1956-1963.
55 Nicolas O, Gavín R, Braun N, *et al*. Bcl-2 overexpression delays caspase-3 activation and rescues cerebellar degeneration in prion-deficient mice that overexpress amino-terminally truncated prion. *FASEB J* 2007; **21**:3107-3117.
56 Parkin ET, Watt NT, Turner AJ, Hooper NM. Dual mechanisms for shedding of the cellular prion protein. *J Biol Chem* 2004; **279**:11170-11178.
57. Marella M, Lehmann S, Grassi J, Chabry J. Filipin prevents pathological prion protein accumulation by reducing endocytosis and inducing cellular PrP release. *J Biol Chem* 2002; **277**:25457-25464.

(**Supplementary information** is linked to the online version of the paper on the *Cell Research* website.)